research papers

Diffraction line profiles from polydisperse crystalline systems

Paolo Scardi* and Matteo Leoni

Dipartimento di Ingegneria dei Materiali, Università di Trento, 38050 Mesiano (TN), Italy.
Correspondence e-mail: paolo.scardi@ing.unitn.it

Diffraction patterns for polydisperse systems of crystalline grains of cubic materials were calculated considering some common grain shapes: sphere, cube, tetrahedron and octahedron. Analytical expressions for the Fourier transforms and corresponding column-length distributions were calculated for the various crystal shapes considering two representative examples of size-distribution functions: lognormal and Poisson. Results are illustrated by means of pattern simulations for a f.c.c. material. Line-broadening anisotropy owing to the different crystal shapes is discussed. The proposed approach is quite general and can be used for any given crystallite shape and different distribution functions; moreover, the Fourier transform formalism allows the introduction in the line-profile expression of other contributions to line broadening in a relatively easy and straightforward way.

1. Introduction

Line broadening is a well known feature of the diffraction profiles from polycrystalline samples. Besides the instrumental contribution, lattice defects (point, line or plane defects) and finite size of coherent diffraction domains are typical sources of line broadening, usually referred to as *strain* and *size* broadening. Line-profile analysis (LPA), as the subject is frequently termed, has been discussed in a remarkable number of papers since 1918 (Scherrer, 1918), including many applications to materials science. Despite the long history, LPA is still the object of active research [for a recent overview, see Snyder *et al.* (1999)].

Conventional methods of LPA (Klug & Alexander, 1974) deal with average size parameters, with little or no information on the actual particle size and shape. This tendency has been so strong that specific methods have been proposed to carry out an analysis independently of the particle shapes (Bertaut, 1949, 1950). This is partly justified by the fact that no physical principle can be invoked *a priori* to establish crystal shapes; in fact, no formal restriction to crystal shape can be related to structure symmetry only (*e.g.* crystals of cubic structure materials need not possess the four threefold axes that pertain to the cubic symmetry). As a consequence, there is no *a priori* knowledge of the shape and size distribution of small crystals: shape and dispersion of sizes in a system of crystalline grains is the result of its history, including preparation techniques and subsequent treatments that the sample under study can have undergone. We can summarize this observation by saying that the shape is not a crystal property, so the Neumann principle[1] does not apply. This prevents us from using simple general-izations based on the crystal symmetry, like those that can be used for lattice strain (Popa, 1998).

However, it is rather frequent (and also favoured by thermodynamic arguments) that small crystalline grains assume simple geometrical shapes, corresponding to those of convex[2] solids [see, for instance, Douvigneaud & Derie (1980), Louër *et al.* (1983), Toraya (1989), Audebrand *et al.* (2000)]. Among these solids, several commonly occurring ones (*e.g.* sphere, cube, tetrahedron and octahedron) can be described by a single length parameter. Other possible crystal shapes (*e.g.* cylinders, prisms or ellipsoids) can include two or more length parameters. Cylinders, for instance, are described by diameter and height; therefore in addition to crystal size an axial ratio (height/diameter) needs to be considered. Consequently, it can be necessary to account for a distribution of shapes as well as for a distribution of sizes. Effects on the diffraction profiles become more difficult to describe, but a LPA is, however, possible (Langford & Louër, 1982; Vargas *et al.*, 1983).

Due consideration should also be given to the fact that, even if diffraction domains have some simple geometrical shape, they rarely have the same size: real systems are more likely to be polydisperse than monodisperse. Recent work tends to include the parameters of a suitable size distribution in the analysis of powder diffraction patterns (Krill & Birringer, 1998; Langford *et al.*, 2000). For instance, a lognormal distribution seems appropriate to several real cases of study (see Langford *et al.*, 2000, and references therein), but once again no *a priori* principle can be invoked in the choice of a size distribution.

A further important feature of the size effects is line-broadening anisotropy, *i.e.* a variation of line broadening with

---

[1] The Neumann principle requests that physical properties include symmetry elements of the crystal point group.

[2] A convex solid is such that the line connecting any two points belongs to the solid.

the scattering direction. Such effects can be more or less pronounced, or absent (for instance, in the case of a system of spheres), depending on the specific crystal shape and parameters of the size distribution. Even if other sources of anisotropy can be present [*e.g.* elastic anisotropy (Stokes & Wilson, 1944)], size anisotropy is rather peculiar, and can be a useful clue for studying crystal shape in highly dispersed systems (Langford, 1992). In addition, a correct consideration of line-broadening anisotropy is important in the many methods relying on pattern modelling or fitting [*e.g.* the Rietveld method (Young, 1993)].

In this work, we consider size effects produced by polydisperse systems, with some representative examples of cubic material grains with single-parameter convex shapes. The Fourier transform formalism developed by Stokes & Wilson (1942, 1944) is used to incorporate the effect of a size distribution into a general analytical expression to be used for simulation or modelling of experimental patterns. Extension to more complex cases (lower symmetry materials and different crystal shapes) can be based on the same proposed approach.

2. Diffraction profile of a system of crystalline grains

The effect of a finite domain size on the diffraction profile can be conveniently studied in terms of the Fourier transform of the scattered intensity. As shown by Wilson (1962), this can be performed in a very general form, also accounting for the presence of lattice defects, and is the basis of a recent algorithm for whole powder pattern modelling (WPPM) (Scardi *et al.*, 2000, 2001*a,b*). The approach described in the following can be used for any crystal shape, but in this work we demonstrate the application to the case of size effects produced by polydisperse systems of crystalline grains of cubic materials with simple convex shapes, whose volume can be described by a single length parameter (*e.g.* sphere diameter or edge for cube, tetrahedron or octahedron). The intensity scattered by a crystal c described by the length parameter D can be written as[3]

$$I_c(s, D) = k(s) \int_0^\infty A_c(L, D) \exp(2\pi iLs) \, \mathrm{d}L, \qquad (1)$$

where $s = 2 \sin\theta/\lambda$ is the reciprocal-lattice variable, L is a length in the real space and $A_c(L, D)$ is the Fourier transform (FT) of the diffraction profile for the crystallite c; $k(s)$ includes constants and trigonometric factors related to the experimental geometry.

Actually, the integration extends up to a finite value of L rather than to infinity, since the crystallite volume and length are in any case finite,

$$I_c(s, D) = k(s) \int_0^{D'(hkl)} A_c(L, D) \exp(2\pi iLs) \, \mathrm{d}L. \qquad (2)$$

D' is a function of (hkl), because the integration limit generally depends on the scattering direction. Usually D' is a simple function of D and h, k, l; without loss of generality, we can write $D' = D/K(hkl)$, where $K(hkl)$ contains the dependence on lattice direction (and hence on the Miller indices) and on the crystallite shape.

If the sample is a polydisperse system, the presence of crystalline grains with the same shape but different size can be described by an appropriate distribution of the length parameter, $g(D)$. The intensity scattered by the system is

$$I(s) = k(s) \frac{\int_0^\infty I_c(s, D)g(D)V_c(D) \, \mathrm{d}D}{\int_0^\infty g(D)V_c(D) \, \mathrm{d}D}, \qquad (3)$$

where $V_c(D)$ is the crystallite volume. If we use (2) in the previous expression, then we obtain

$$I(s) = k(s) \int_{D=0}^\infty \int_{L=0}^{D/K} A_c(L, D) \exp(2\pi iLs) \, \mathrm{d}Lw(D) \, \mathrm{d}D$$
$$\times \left[\int w(D) \, \mathrm{d}D \right]^{-1}, \qquad (4)$$

where the weight function $w(D) = g(D)V_c(D)$ was introduced. By swapping the integration order,

$$I(s) = k(s) \int_{L=0}^\infty \int_{D=LK}^\infty A_c(L, D)w(D) \, \mathrm{d}D \exp(2\pi iLs) \, \mathrm{d}L$$
$$\times \left[\int w(D) \, \mathrm{d}D \right]^{-1}. \qquad (5)$$

If we define the FT for the system of crystallites as

$$A(L) = \frac{\int_{LK}^\infty A_c(L, D)w(D) \, \mathrm{d}D}{\int w(D) \, \mathrm{d}D}, \qquad (6)$$

then the intensity scattered by the sample can be written as

$$I(s) = k(s) \int_0^\infty A(L) \exp(2\pi iLs) \, \mathrm{d}L. \qquad (7)$$

This is a rather general result; changing the crystallite shape or $g(D)$ only requires recalculation of the FT by means of (6).

3. Fourier transform of the intensity scattered by a small crystal

$A(L)$ can be calculated by using the 'ghost' concept introduced by Stokes & Wilson (1942). Essentially, the FT is proportional to the volume shared by the crystal and its 'ghost', *i.e.* an equivalent crystal (same shape and size) shifted a distance L along the scattering direction. As shown by Wilson (1962) for the crystal shapes considered here,[4] the FT is given by a polynomial of third degree, whose coefficients can be worked out on the basis of simple geometrical considerations (Wilson, 1962). Other shapes have been proposed in the literature, but they will not be considered here since they

---

[3] Since $A_c(L, D)$ are even functions in L, the scattered intensity can be written as cosine FT as far as *size* effects only are considered. An advantage of the complex notation is that the formalism can more readily be adapted to include line broadening from other sources (*e.g.* faulting and line defects).

[4] The FT can be written as a third-degree polynomial of the Fourier length L for any polyhedron (in addition to spheres). For a demonstration, see Appendix A.

research papers

involve more than one dimensional parameter [*e.g.* hexagonal prisms (Vargas *et al.*, 1983) and cylinders (Langford & Louër, 1982)].

For a sphere of diameter D, the FT is given by

$$A_{\text{Sph}}(L, D) = 1 - \frac{3}{2}\frac{L}{D} + \frac{1}{2}\frac{L^3}{D^3} \quad \text{for} \quad 0 \leq L \leq D \quad (K = 1). \tag{8}$$

For a spherical crystallite, it is not necessary to know the crystal symmetry and orientation, which on the contrary need be specified for other crystallite shapes. In the following, we conveniently choose to index reflections using positive indices with $h \geq k \geq l$. For a cubic crystallite delimited by {100} faces, the FT is given by

$$A_{\text{Cub}}(L, D) = \left(1 - A\frac{L}{D}\right)\left(1 - B\frac{L}{D}\right)\left(1 - C\frac{L}{D}\right) \quad \text{for} \quad 0 \leq L \leq D', \tag{9}$$

where D is the cube edge and $A = h/(h^2 + k^2 + l^2)^{1/2}$, $B = k/(h^2 + k^2 + l^2)^{1/2}$, $C = l/(h^2 + k^2 + l^2)^{1/2}$. D' depends on the scattering direction and, according to our choice for the Miller indices, $D' = D/A$ [$K(hkl) = A$].

For tetrahedral and octahedral crystals, the FT depends on the scattering direction, and in particular on the sign of $h - (k + l)$ [or equivalently $A - (B + C)$]. Following Stokes & Wilson (1942), we assume that the tetrahedron is bounded by (111), $(1\bar{1}\bar{1})$, $(\bar{1}1\bar{1})$, $(\bar{1}\bar{1}1)$ planes, whereas octahedral crystals are bounded by the eight {111} planes. For a tetrahedron, we can write

$$A_{\text{Tet}}(L, D) = \left(1 - 2^{1/2}A\frac{L}{D}\right)^3$$
$$\text{for} \quad 0 \leq L \leq D/(2^{1/2}A), \quad h \geq k + l, \tag{10a}$$

$$A_{\text{Tet}}(L, D) = \left(1 - \frac{A + B + C}{2^{1/2}}\frac{L}{D}\right)^3$$
$$\text{for} \quad 0 \leq L \leq 2^{1/2}D/(A + B + C), \quad h \leq k + l. \tag{10b}$$

Consequently, $K = 2^{1/2}A$ for $h \geq k + l$ and $K = (A + B + C)/2^{1/2}$ for $h \leq k + l$.

For octahedral crystals,

$$A_{\text{Oct}}(L, D) = 1 - \frac{3 \times 2^{1/2}}{2}A\frac{L}{D} + \frac{3}{2}(A^2 - B^2 - C^2)\left(\frac{L}{D}\right)^2$$
$$+ \frac{1}{2 \times 2^{1/2}}[-A^3 + 3A(B^2 + C^2) + 2(B^3 + C^3)]$$
$$\times \left(\frac{L}{D}\right)^3$$
$$\text{for} \quad 0 \leq L \leq \frac{2^{1/2}D}{A + B + C}, \quad h \geq k + l, \tag{11a}$$

$$A_{\text{Oct}}(L, D) = 1 - \frac{1}{2^{1/2}}(2A + B + C)\frac{L}{D}$$
$$+ \frac{1}{4}[A^2 - 3(B - C)^2 + 2A(B + C)]\left(\frac{L}{D}\right)^2$$
$$+ \frac{1}{4 \times 2^{1/2}}(A + B + C)[A^2 + 3(B - C)^2]\left(\frac{L}{D}\right)^3$$
$$\text{for} \quad 0 \leq L \leq \frac{2^{1/2}D}{A + B + C}, \quad h \leq k + l \tag{11b}$$

and $K = (A + B + C)/2^{1/2}$ in both cases.

In a general form, the above FTs can be written as

$$A_c(L, D) = \sum_{n=0}^{3} H_n^c(L/D)^n, \tag{12}$$

where the polynomial coefficients are reported in Table 1. From the above expression, it is also possible to calculate crystallite apparent sizes [or mean column length (MCL)] defined as[5]

$$\langle L \rangle_s = -\left[\frac{dA_c(L, D)}{dL}\bigg|_{L=0}\right]^{-1} \quad \text{(area-weighted MCL)} \tag{13a}$$

$$\langle L \rangle_v = [\beta(s)]^{-1} = 2 \int_0^{D/K} A_c(L, D)\, dL$$
$$\text{(volume-weighted MCL)}, \tag{13b}$$

where $\beta(s)$ is the integral breadth in the reciprocal lattice. By using (12) in the two previous equations, it is then possible to obtain general formulae for MCLs,

$$\langle L \rangle_s = \frac{D}{K_\kappa} = -\frac{D}{H_1}, \tag{14a}$$

$$\langle L \rangle_v = \frac{D}{K_\beta} = \frac{D\{3H_3 + 2K[2H_2 + 3K(H_1 + 2KH_0)]\}}{6K^4}, \tag{14b}$$

where K_β and K_κ are the integral breadth and the initial-slope Scherrer constants, respectively. Further useful relations on Scherrer constants and MCLs can be found in the exhaustive publication of Langford & Wilson (1978).

4. Size distributions

As discussed briefly in the *Introduction*, a lognormal size distribution frequently proved to be appropriate in practical cases, like highly dispersed ceramic powders produced by chemical methods (*e.g.* sol–gel), or in catalysts; such a distribution was also observed in highly deformed metal grains (see Langford *et al.*, 2000, and references therein). A lognormal is described by two parameters, μ and σ, the *lognormal mean* and *variance*, respectively.

$$g_l(D) = \frac{1}{D\sigma(2\pi)^{1/2}}\exp[-(\ln D - \mu)^2/2\sigma^2]. \tag{15}$$

---

[5] Volume-weighted MCL and area-weighted MCL are also referred to as integral breadth apparent size (ε_β) and Fourier apparent size (ε_F), respectively (Langford & Wilson, 1978).

Table 1
H_n, K^c (hkl) coefficients for sphere, cube, tetrahedron and octahedron.

	Sphere	Cube	Tetrahedron		Octahedron	
			$A \geq B + C$†	$A \leq B + C$	$A \geq B + C$	$A \leq B + C$
H_0	1	1	1	1	1	1
H_1	$-3/2$	$-(A + B + C)$	$-3 \times 2^{1/2}A$	$-3(A + B + C)/2^{1/2}$	$-3A/2^{1/2}$	$-(2A + B + C)/2^{1/2}$
H_2	0	$AB + BC + CA$	$6A^2$	$3(A + B + C)^2/2$	$3(A^2 - B^2 - C^2)/2$	$[A^2 - 3(B - C)^2 + 2A(B + C)]/4$
H_3	$1/2$	$-ABC$	$-2 \times 2^{1/2}A^3$	$-(A + B + C)^3/(2 \times 2^{1/2})$	$[-A^3 + 3A(B^2 + C^2) + 2(B^3 + C^3)]$ $\times (2 \times 2^{1/2})^{-1}$	$\{(A + B + C)[A^2 + 3(B - C)^2]\}$ $\times (4 \times 2^{1/2})^{-1}$
$K^c(hkl)$	1	A	$2^{1/2}A$	$(A + B + C)/2^{1/2}$	$(A + B + C)/2^{1/2}$	$(A + B + C)/2^{1/2}$

† The conditions: $h \geq k + l$, $h \leq k + l$ are equivalent, respectively, to $A \geq B + C$, $A \leq B + C$.

μ and σ should not be confused with the equivalent quantities for the distribution, which can be obtained from the central moments of the lognormal distribution ($M_{l,n}$), given by

$$M_{l,n} = \exp[n\mu + (n^2/2)\sigma^2].\qquad(16)$$

Consequently, mean size and variance are defined as

$$M_{l,1} = \exp\left(\mu + \tfrac{1}{2}\sigma^2\right) \qquad \text{(mean)}\qquad(17a)$$

$$M_{l,2} - (M_{l,1})^2 = \exp(2\mu + \sigma^2)[\exp(\sigma^2) - 1] \qquad \text{(variance)}.\qquad(17b)$$

The approach proposed in this work can be developed for any other distribution function. As an example of an alternative to the lognormal, to model polydisperse systems with different features we can consider a Poisson distribution, $g_p(D)$, defined as[6]

$$g_p(D) = \frac{\gamma}{M_{p,1}\Gamma(\gamma)}\left(\frac{\gamma D}{M_{p,1}}\right)^{\gamma - 1}\exp(-\gamma D/M_{p,1}),\qquad(18)$$

where $M_{p,1}$ is the mean, whereas γ is the ratio between mean square and variance: $\gamma = M_{p,1}^2/(M_{p,2} - M_{p,1}^2)$. The general formula for the moments of the Poisson distribution ($M_{p,n}$) is given by

$$M_{p,n} = \left(\frac{M_{p,1}}{\gamma}\right)^n \frac{\Gamma(n + \gamma)}{\Gamma(\gamma)}.\qquad(19)$$

Recently, it was shown that the lognormal distribution moments of the second, third and fourth order can be related to $\langle L \rangle_S$ and $\langle L \rangle_V$ for a polydisperse system of spheres (Krill & Birringer, 1998; Langford, et al., 2000),

$$\langle L \rangle_{l,S} = \tfrac{2}{3}\frac{M_{l,3}}{M_{l,2}} = \tfrac{2}{3}\exp[\mu_l + (5/2)\sigma_l^2],\qquad(20a)$$

$$\langle L \rangle_{l,V} = \tfrac{3}{4}\frac{M_{l,4}}{M_{l,3}} = \tfrac{3}{4}\exp[\mu_l + (7/2)\sigma_l^2].\qquad(20b)$$

These relations have the practical utility to directly connect distribution parameters and effective crystallite sizes. As recognized by Langford & Wilson (1978), this result has a more general validity. In fact, the presence of a size distribution does not alter the relation between crystal shape and line profile; for the MCLs, this relation is in any case expressed by

[6] The *incomplete gamma function* is defined as $\Gamma(x, a) = \int_a^\infty y^{x-1}\exp(-y)\,\mathrm{d}y$. The *gamma function*, $\Gamma(x)$, is obtained for $a = 0$.
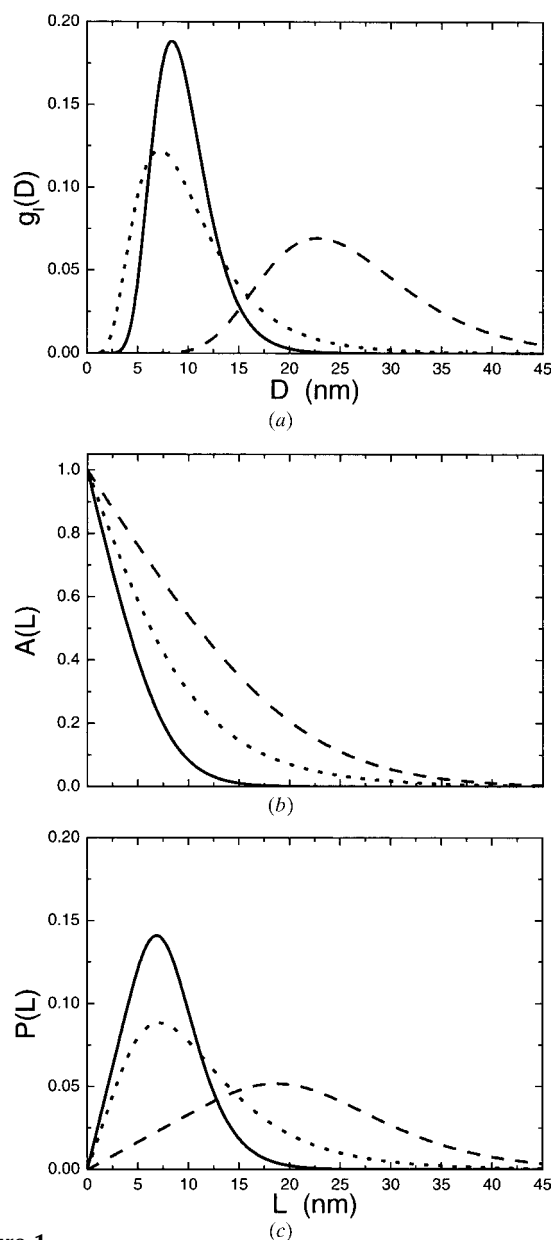
Figure 1
(a) Lognormal distributions of diameters for a system of spherical crystallites, $g_l(D)$, (b) with corresponding Fourier transforms $A(L)$, and (c) column-length distributions $P(L)$, for different choices of lognormal mean (μ) and variance (σ): $\mu = 2$, $\sigma = 0.3$ (line), $\mu = 2$, $\sigma = 0.5$ (dot), $\mu = 3$, $\sigma = 0.3$ (dash).

the Scherrer constants, and the general expressions for poly-disperse systems read

$$\langle L \rangle_S = \frac{1}{K_k} \frac{M_3}{M_2}, \qquad (21a)$$

$$\langle L \rangle_V = \frac{1}{K_\beta} \frac{M_4}{M_3}. \qquad (21b)$$

K_k and K_β can be found in Langford & Wilson (1978) or, for the crystal shapes considered in this work, from equation (14a,b). Apparent sizes can then be calculated for any desired size distribution, in terms of distribution moments and Scherrer constants.

5. Fourier transform for a system of crystals

The general expression for the FT of the scattered intensity from a system of crystals with the same shape and a distribution of sizes is equation (6). For a given choice of crystal shape (in the present work, defined through the H_n coefficients of Table 1), the FT depends on the size-distribution parameters only,

$$A(L) = \frac{\int_{LK}^{\infty} A_c(L, D) D^3 g(D) \, \mathrm{d}D}{\int_0^{\infty} D^3 g(D) \, \mathrm{d}D}. \qquad (22)$$

The normalization integral in the denominator is the distribution moment of third order $\{M_3 = \exp[3\mu + (9/2)\sigma^2]$ for a
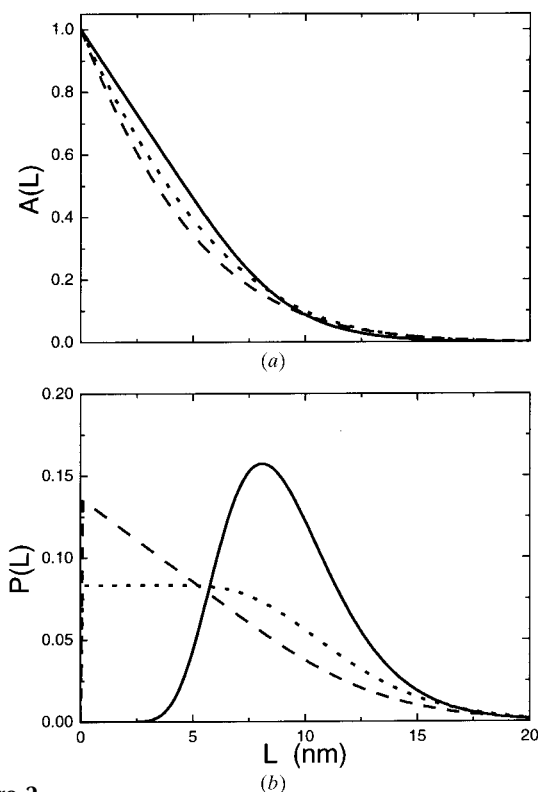

Figure 2
(a) Fourier transforms and (b) corresponding column-length distributions for a system of cubic crystallites (lognormal distribution of cube edges, with $\mu = 2$, $\sigma = 0.3$) for different diffraction peaks: (h00) (line), (hh0) (dot), (hhh) (dash).

lognormal}. For the crystal shapes considered in this work, $A_c(L, D)$ is a polynomial [equation (12)]; the H_n coefficients can be factorized and the above integral can be solved by parts.[7] In the case of a lognormal distribution, we can write the following general formula:

$$A_l(L) = \sum_{n=0}^{3} H_n^c \, \mathrm{erfc}\left[\frac{\ln(LK^c) - \mu - (3 - n)\sigma^2}{\sigma 2^{1/2}}\right] \frac{M_{l,3-n}}{2M_{l,3}} L^n. \qquad (23)$$

This expression can be used in equation (7) to calculate the diffraction profile, which can then be expressed in terms of lognormal mean and variance, also accounting for crystallite shape and consequently size anisotropy, through the crystal parameters H_n^c and K^c.

For a comparison among different grain shapes it is appropriate to define an effective size parameter as $D_{\mathrm{Vol}} = [V_c(D)]^{1/3}$, where D is the actual size parameter (diameter for sphere and edge for cube, tetrahedron and octahedron) (Wilson, 1962). If we use D_{Vol} instead of D in the size distribution, then we can compare systems of crystals with different shapes but same average volume in order to single out the anisotropy effect characteristic of each crystal shape. As an example of the application of (23), Fig. 1 shows three different lognormal distributions with the corresponding FTs for sphere systems. By varying the lognormal parameters, we can change the shape of the distribution (width and mean value) and change the FT accordingly.

Size anisotropy effects can be appreciated by plotting the FTs for the different crystal shapes with a given choice of lognormal parameters ($\mu = 2$, $\sigma = 0.3$, cf. Fig. 1). This is shown in Figs. 2, 3 and 4 (for cubes, tetrahedra and octahedra, respectively) along three representative directions [(h00), (hh0) and (hhh)] in cubic systems.

As pointed out previously, the presence of a size distribution does not alter the size anisotropy effect. A further means to illustrate this point is by considering the Williamson–Hall (WH) plot (Langford, 1992) for the different crystal shapes. We can conveniently plot the integral breadth [from equation (13b)] as a function of $(h^2 + k^2 + l^2)^{1/2}$, which is proportional to the reciprocal-space variable $[s = (1/a)(h^2 + k^2 + l^2)^{1/2},$ where a is the lattice parameter]; this is shown in Fig. 5 for a f.c.c. material. Oscillations in the corresponding trends shown in Fig. 5 do not depend on the dispersion degree but on the crystal shape only, with the distribution parameters simply scaling the $\beta(s)$ value. These features of the size-broadening effect should be carefully considered in the analysis of real materials, where oscillations in the WH plot can also be attributed to lattice defects or to experimental errors.

---

[7] The integral can be easily solved considering

$$\int_x^{\infty} \exp(zt) \frac{1}{\omega(2\pi)^{1/2}} \exp\left[\frac{-(t - \gamma)^2}{2\omega^2}\right] \mathrm{d}t$$

$$= \frac{1}{2} \exp\left(\gamma z + \frac{\omega^2 z^2}{2}\right) \mathrm{erfc}\left(\frac{x - \gamma - z\omega^2}{2^{1/2}\omega}\right).$$

Size anisotropy and dispersion effects are quite evident in a powder pattern. Fig. 6(*a*) shows simulated patterns for a f.c.c. material with lattice parameter $a = 0.5411$ nm (cerium oxide) using Cu $K\alpha$ radiation, considering systems of spheres, cubes, tetrahedra and octahedra with the distribution parameters of Figs. 2, 3 and 4. From these patterns, and the detail for the (111) and (200) profiles in Fig. 6(*b*), we can appreciate the close similarity between size effects produced by spheres (isotropic) and octahedra (weakly anisotropic); much stronger is the anisotropy effect of cubic or of tetrahedral crystal shapes.

The simulation for the sphere system is equivalent to that recently obtained by Langford, Louer & Scardi (2000) (LLS), who considered the same type of system (lognormal distribution of spheres) and proposed a modelling based on Wilson's expression for the diffraction profile from a single crystal [equation (24) of Wilson (1962)]. This is not surprising, as the two approaches (the present one and LLS) have a common basis: according to LLS, the observed diffraction pattern can be modelled by the sum, weighted on $w(D)$, of the diffraction profiles from crystallites with different diameters. This is equivalent to equation (3), which is a basic assumption of the present FT model.

A procedure analogous to that shown for a lognormal distribution leads to the FT for a system of crystals with the size parameter distributed according to a Poissonian,

$$A_p(L) = \sum_{n=0}^{3} H_n^c \left(\frac{\gamma}{M_{p,1}}\right)^n \frac{\Gamma[\gamma + (3 - n), (K^c L \gamma / M_{p,1})]}{\Gamma(\gamma + 3)} L^n.$$

(24)

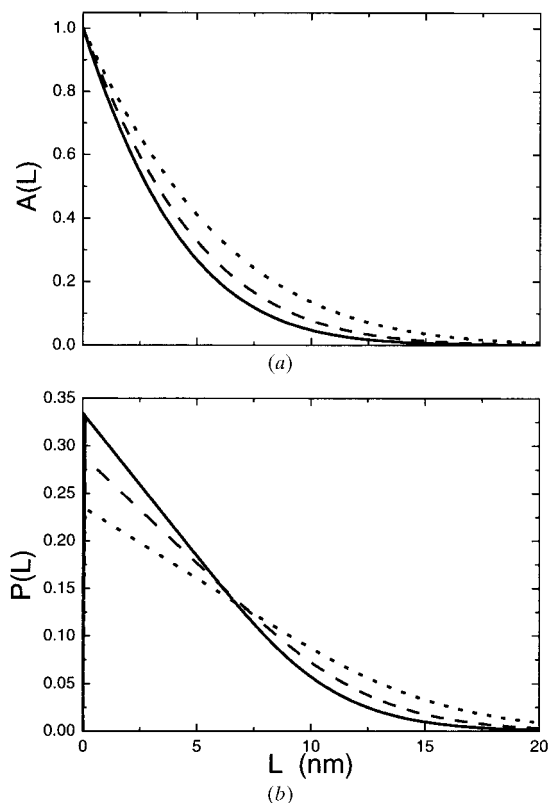Equation (24), like the corresponding expression for the lognormal distribution, can be used to simulate or to model
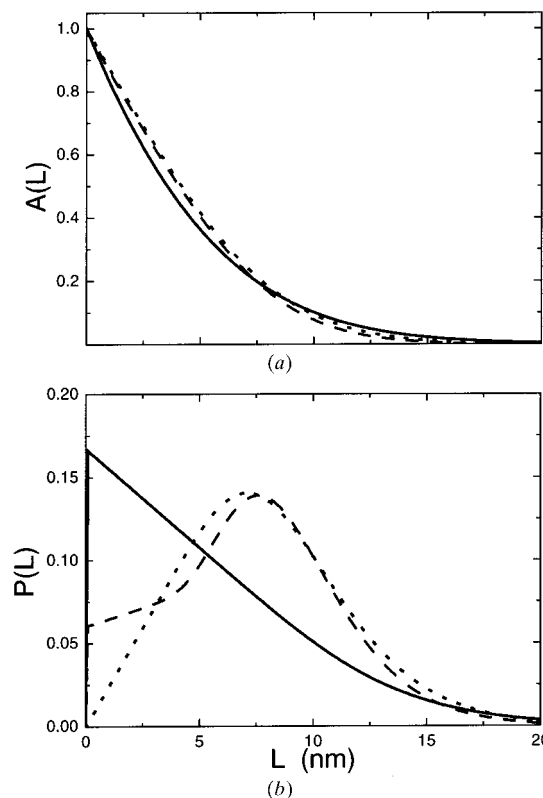
Figure 4
(*a*) Fourier transforms and (*b*) corresponding column-length distributions for a system of octahedral crystallites (lognormal distribution of octahedron edges, with $\mu = 2$, $\sigma = 0.3$) for different diffraction peaks: (*h*00) (line), (*hh*0) (dot), (*hhh*) (dash).

Figure 3
(*a*) Fourier transforms and (*b*) corresponding column-length distributions for a system of tetrahedral crystallites (lognormal distribution of tetrahedron edges, with $\mu = 2$, $\sigma = 0.3$) for different diffraction peaks: (*h*00) (line), (*hh*0) (dot), (*hhh*) (dash).
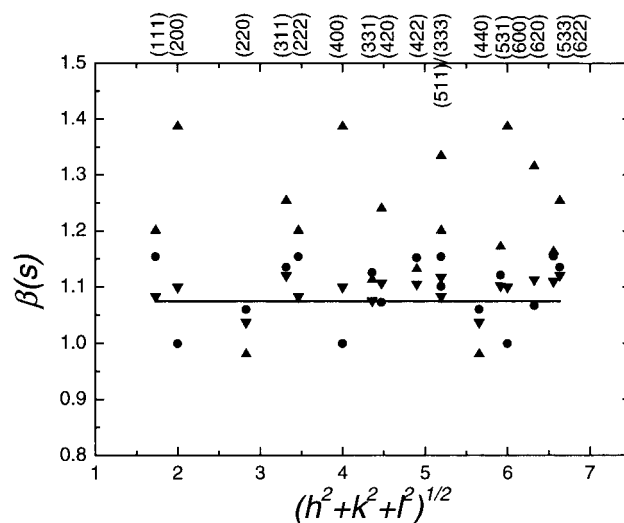
Figure 5
Williamson–Hall plot for a f.c.c. material with lattice parameter $a = 0.5411$ nm (cerium oxide) for systems of spheres (line), cubes (circle), tetrahedra (upward triangle) and octahedra (downward triangle).

diffraction patterns and for additional discussion as performed with equation (23). Since we do not expect changes in the size anisotropy effects (*cf.* §4), there is no point in replicating simulations for the Poisson distribution case. An interesting feature of the Poisson distribution that is worth noting here is the considerable change of shape, and correspondingly different diffraction profiles, resulting from a change of variance. This is shown in Fig. 7, where $g_p(D)$ is plotted for a fixed mean ($M_{p,1}$ = 5 nm) and different γ, together with corresponding FTs and simulated profiles [(111) and (200)] for a system of spheres. The high flexibility of the Poisson distribution, which gradually changes from an exponential ($\gamma = 1$) to a Gaussian (in the limit of $\gamma \to \infty$), can be conveniently exploited in the modelling of real size distributions.

As a concluding remark, the advantage of the presented FT-based approach over the LLS approach is the possibility to easily include other effects contributing to the diffraction profile, like the instrumental broadening and the broadening due to lattice defects [*e.g.* dislocation and faulting (Scardi *et al.*, 2000, 2001*a*)]. This is the basis of the recently proposed WPPM (Scardi *et al.*, 2000, 2001*a,b*). As anticipated in §2, a general expression for the diffraction profile can be written in terms of the FT, including size, strain and instrument as

$$I(s) = k(s) \int A^S(L)A^F(L)A^D(L)A^I(L) \exp(2\pi iLs)\,\mathrm{d}L, \quad (25)$$

where suitable expressions for A^S, A^F and A^D [for crystallite size, (twin and deformation) faulting and for dislocations, respectively] are given by Scardi & Leoni (1999) and by Scardi *et al.* (2000, 2001*a*). A^I can be obtained as a FT of a suitable analytical function describing the instrumental profile in an appropriately wide angular range (Leoni *et al.*, 1998; Scardi & Leoni, 1999), or it can be evaluated by using a fundamental parameter approach (Cheary & Coehlo, 1992). The results of the present work evidently concern A^S; a more detailed discussion and applications of equation (25) can be found elsewhere (Scardi *et al.*, 2000, 2001*a,b,c*).

6. Column-length distributions for a system of convex crystals

So far we have shown expressions for the FT of the intensity scattered by polydisperse systems. All the information concerning size broadening is included in the FT: in fact, we can simulate or model diffraction profiles, and also calculate mean effective size values (MCLs) and profile widths. A further concept frequently used in LPA is column length distribution (CLD), $p(L)$. Although unnecessary in the present context, it can be useful to calculate the CLD for the systems of crystal considered in this work, to discuss some features of $p(L)$ that are frequently proposed in the literature. The CLD was originally proposed by Bertaut (1949, 1950) to represent the FT in terms of a distribution function of column lengths along the scattering direction; it can be defined as (Warren, 1969)

$$A(L) = \frac{1}{\langle L \rangle_S} \int\limits_{|L|}^{\infty} (L' - |L|)p(L')\,\mathrm{d}L', \quad (26)$$

with the normalization condition $\int_0^\infty p(L)\,\mathrm{d}L = 1$. Under suitable conditions [$(\mathrm{d}^2 A(L)/\mathrm{d}L^2) \geq 0$] (Bertaut, 1950), it is possible to show that the CLD is proportional to the second derivative of the FT with respect to L. Therefore, we can use equation (23) or (24) to calculate $P(L)$, the CLD for a polydisperse system of spheres, cubes, tetrahedra or octahedra. The expressions obtained for a lognormal and for a Poisson distribution, respectively, are the following (an alternative approach is shown in Appendix *B*):

$$P_l(L) = \sum_{n=0}^{3} \frac{H_n^c}{H_1^c} \left(n(1-n)\,\mathrm{erfc}\left[\frac{\ln(LK^c) - \mu - (3-n)\sigma^2}{\sigma 2^{1/2}} \right] \right.$$
$$+ \frac{1}{\sigma^3}\left(\frac{2}{\pi}\right)^{1/2} [-\ln(LK^c) + \mu + (2+n)\sigma^2]$$
$$\left. \times \exp\left\{ -\left[\frac{\ln(LK^c) - \mu - (3-n)\sigma^2}{\sigma 2^{1/2}} \right]^2 \right\} \right) \frac{M_{3-n}}{2M_2} L^{n-2}$$
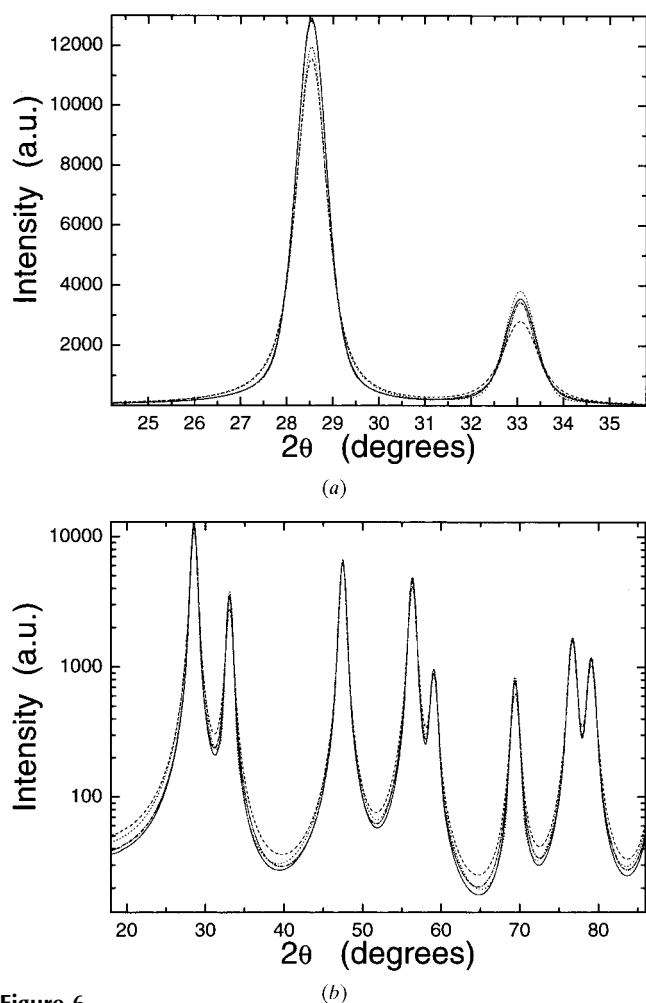
$$(27)$$

Figure 6
(*a*) Simulated patterns (for a f.c.c. material using Cu Kα radiation) corresponding to the conditions used for Fig. 1 ($\mu = 2$, $\sigma = 0.3$) for spheres (line), Fig. 2 for cubes (dot), Fig. 3 for tetrahedra (dash) and Fig. 4 for octahedra (dash–dot) on log scale; (*b*) detail of (*a*) on linear scale.

$$P_p(L) = \sum_{n=0}^{3} \frac{H_n^c}{H_1^c} \Big(n(n-1)\Gamma[\gamma + (3-n), (K^c L\gamma/M_{p,1})]$$
$$+ \{\exp(-K^c L\gamma/M_{p,1})(K^c L\gamma/M_{p,1})^{\gamma+(3-n)}$$
$$\times [1 - \gamma - (3-n) + (K^c L\gamma/M_{p,1}) - 2n]\}\Big)$$
$$\times (2+\gamma)(\gamma/M_{p,1})^{n-1} L^{n-2}. \tag{28}$$

Examples of the use of equations (27) and (28) are reported in Figs. 1 to 7 for different crystal shapes and size distributions.

It is quite evident from these examples that it is not generally possible to use simple analytical functions to model the CLD. Different crystal shapes lead to remarkably different CLDs (and diffraction profiles), and the anisotropy effect also can be a relevant effect. For instance, the use of an exponential function [$\exp(-L/M)$], frequently proposed as a simple CLD model, does not seem justified; even in the isotropic case of spherical crystallites, the actual CLD is far from an exponential. This point needs to be underlined since the frequently used WH plot is based on the assumption of a Lorentzian *size* profile component, which is equivalent to saying that the CLD is an exponential. In spite of the usefulness of the WH plot to draw preliminary conclusions on LPA, its numerical results should not be considered seriously, unless very specific

assumptions justify the use of an exponential CLD [further approximations in the WH plot also concern the *strain* broadening contribution (Langford, 1992)].

The results reported so far illustrate how the diffraction pattern from systems of crystals with a distribution of sizes can be easily modelled by using the FT of the scattered intensity. However, it is useful to remember some limits of this approach. Primarily, it should always be borne in mind that we approximated the discrete distribution of scattering centres (which physically produce the diffracted signal) by a continuous distribution function for lattice cells; this approximation, implicit in the ghost concept of Wilson (1962), becomes progressively less valid by reducing the crystallite size. It is therefore likely that the diffracted signal from very small crystals is not correctly reproduced by the FT approach.

7. Conclusions

The Fourier transform formalism provides an effective means to calculate diffraction line profiles of polydisperse crystalline systems. Simple FT expressions can be derived for most common crystal shapes, profiting from the fact that the FT of the intensity scattered by spherical or polyhedral crystals is a cubic polynomial of the Fourier length. The effect of a size
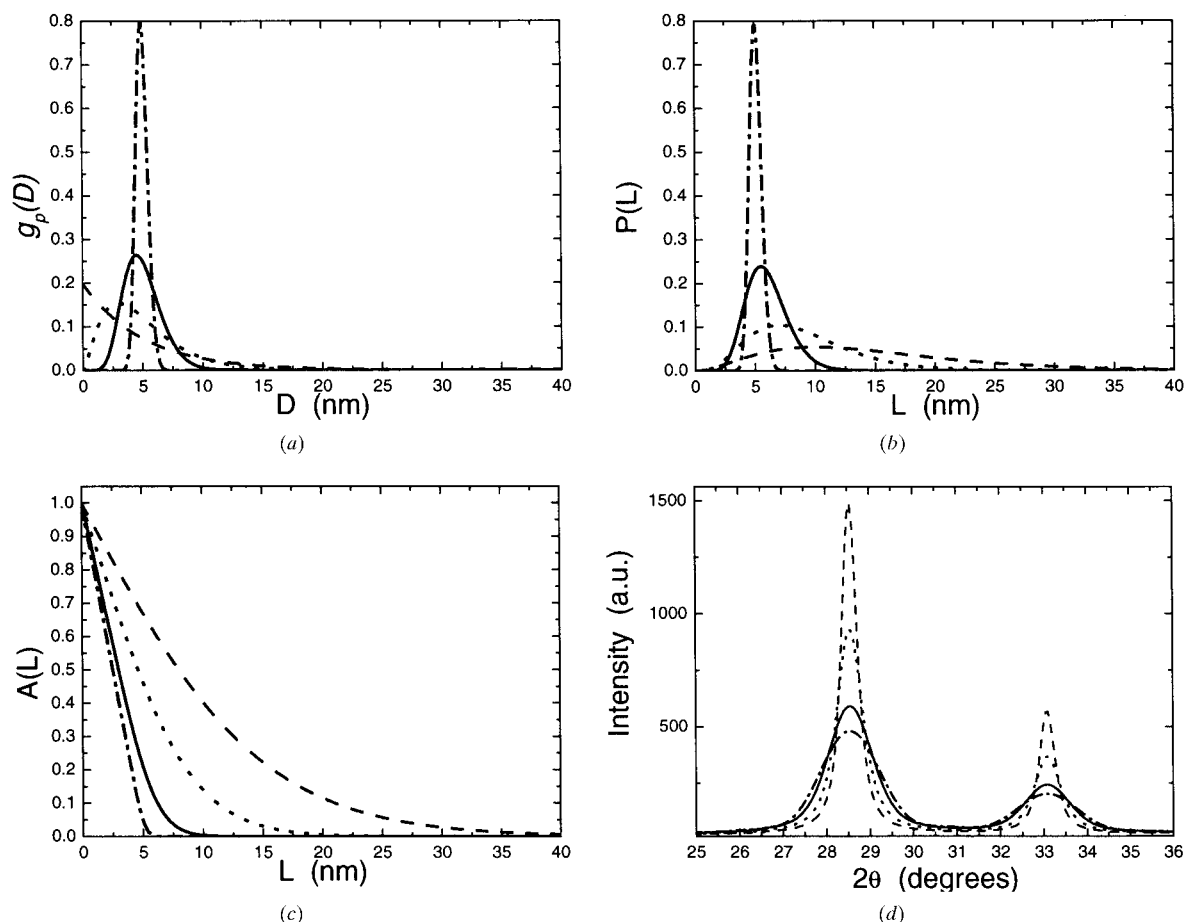

Figure 7
(a) Poisson distributions of diameters for a system of spherical crystallites, $g_p(D)$, with fixed mean (5 nm) and different variance [$\sigma = 1$ (dash), $\sigma = 2.5$ (dot), $\sigma = 10$ (line), $\sigma = 100$ (dash-dot)]; (b) corresponding column-length distributions; (c) Fourier transforms; and (d) simulated diffraction profiles [(111 and (200) peaks for a f.c.c. material, using Cu $K\alpha$ radiation].

dispersion can be introduced in the analysis by an integration of the single-crystal FT weighted over an appropriate grain-size distribution (*e.g.* a lognormal or a Poissonian). Analytical expressions can be obtained for the FT of polydisperse systems and for the corresponding column-length distributions.

Line broadening owing to domain size, including the anisotropy effects owing to the crystal shape, is clearly visible in simulated patterns derived from analytical FT expressions. An interesting feature of the present approach is the possibility to add domain size-related effects to a general expression for the diffraction line profiles including other physical effects as well as instrumental factors. In this way, the diffraction pattern of polycrystalline materials can be modelled without using arbitrary profile-shape functions, directly refining physical parameters related to line-broadening sources.

APPENDIX *A*
Fourier transform of the intensity scattered by a polyhedral crystal

The FT of the intensity scattered by any polyhedral crystal is proportional to the intersection volume (IV) between the polyhedron and its ghost, an equal polyhedron shifted by L along the scattering direction s. The proportionality constant is the polyhedron volume; therefore the FT is unity for $L = 0$ and it is zero for $L \geq L_{max}$, the maximum length of the crystal along s.

We can prove, by simple geometrical reasoning, that the IV (and thus the FT) of any polyhedral crystal is a third-degree polynomial function of L. If the polyhedron is non-convex, the FT can be discontinuous but still a piecewise third-degree polynomial; we can therefore limit ourselves to the convex case.

We can subdivide a polyhedral crystal into a suitable (finite) number of tetrahedra. Without loss of generality, the tetrahedra can be chosen with one face perpendicular to the scattering direction. Consequently, the demonstration reduces to show that the IV for any of these tetrahedra is a cubic polynomial of L.

We can conveniently choose a coordinate system with the z axis parallel to the scattering direction (see Fig. 8), for which a generic tetrahedron T with one face perpendicular to s is described by the following four points: $P_1 = (x_1, y_1, 0)$, $P_2 = (x_2, y_2, 0)$, $P_3 = (x_3, y_3, 0)$, $P_4 = (x_4, y_4, z_4)$.

The volume of T can be obtained by the well known determinant formula,

$$V_T = \frac{1}{6} \begin{vmatrix} x_1 - x_2 & y_1 - y_2 & 0 \\ x_1 - x_3 & y_1 - y_3 & 0 \\ x_1 - x_4 & y_1 - y_4 & -z_4 \end{vmatrix}$$
$$= |[x_1(y_2 - y_3) + x_2(y_3 - y_1) + x_3(y_1 - y_2)]z_4|. \quad (29)$$

Analogously, the IV is given by

$$\mathrm{IV}(L) = \left| \left(1 - \frac{L}{2z_4} + \frac{L^2}{2z_4^2} - \frac{L^3}{6z_4^3} \right) V_T \right|. \quad (30)$$

Consequently, the FT $[\mathrm{IV}(L)/V_T]$ is also a cubic polynomial.

APPENDIX *B*
Column-length distribution for a system of spheres

As an alternative to the procedure illustrated in the above paragraphs, the CLD for a polydisperse system can be calculated from the CLD of a single crystal with a given geometrical shape. For simplicity, we still consider the case of a system of crystals with one size parameter distributed according to $g(D)$. If $p(L)$ for a given crystal shape is available, the colum-length distribution $P(L)$ for a system of crystals is given by

$$P(L) = \frac{\int_{LK}^{\infty} g(D)p'(L, D)\,\mathrm{d}D}{\int_0^{\infty} \int_{LK}^{\infty} g(D)p'(L, D)\,\mathrm{d}D\,\mathrm{d}L}$$
$$= \frac{\int_{LK}^{\infty} g(D)p'(L, D)\,\mathrm{d}D}{\int_0^{\infty} g(D)\int_0^{D/K} p'(L, D)\,\mathrm{d}L\,\mathrm{d}D}, \quad (31)$$

where the CLD for a single crystal is replaced by $p'(L, D) = D^2 p(L, D)$, since the contribution from each crystal must be weighted on its cross section (constant terms are omitted). Equation (31) gives the same result as that obtained by taking the second derivative of the FT. However, if one wishes to use $P(L)$ to calculate the FT for a polydisperse system [by means of equation (26)], integration is more cumbersome than that of equation (6), even if, also in this case, we obtain the same result. In general, it seems preferable to adopt the procedure delineated in the present work, *i.e.* to work out the FT starting
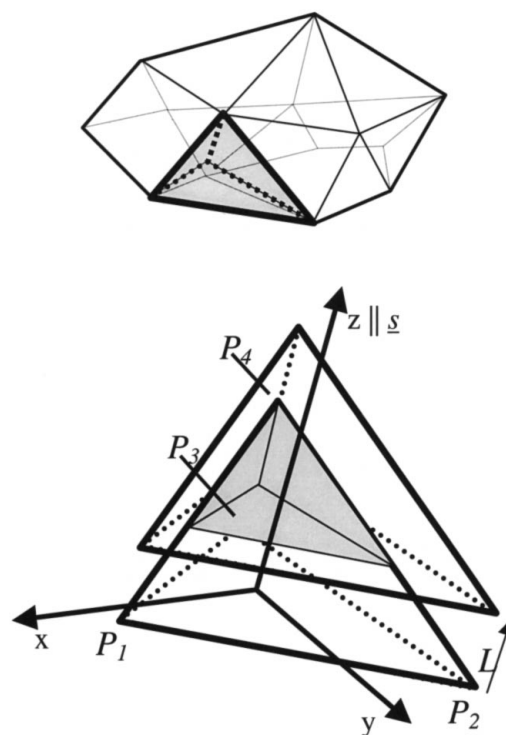

Figure 8
Polyhedral crystal (top). The polyhedron can be subdivided into tetrahedra; one of these tetrahedra with a face perpendicular to s is highlighted. The same (enlarged) tetrahedron is shown with its ghost and IV (shaded volume) below. Points P_1–P_4 are also indicated.

from the FT for a single crystal, which can be easily obtained by means of the ghost concept.

As a final remark concerning CLDs, it is important to consider that equation (26) is written for the [00l] direction. If one wishes to use this approach to calculate the FT for a single crystal along a different direction and for one of the shapes discussed in this work, then the upper limit is finite and is equal to $D' = D/K$. Consequently,

$$A_c(L, D) = \frac{1}{\langle L \rangle_S} \int_{|L|}^{D/K(hkl)} (L' - |L|) p(L', D) \, dL'. \tag{32}$$

The authors are especially grateful to Professor B. Firmani and Dr J. I. Langford for the many discussions and useful suggestions.

References

Audebrand, N., Auffredic, J.-P. & Louër, D. (2000). *Chem. Mater.* **12**, 1791–1799.
Bertaut, E. F. (1949). *C. R. Acad. Sci. Paris*, **228**, 187–189, 492–494.
Bertaut, E. F. (1950). *Acta Cryst.* **3**, 14–18.
Cheary, R. W. & Coehlo, A. A. (1992). *J. Appl. Cryst.* **25**, 109–120.
Douvigneaud P. H. & Derie, R. (1980). *J. Solid State Chem.* **34**, 323–333.
Klug, H. P. & Alexander, L. E. (1974). *X-ray Diffraction Procedures for Polycrystalline and Amorphous Materials*. New York: Wiley.
Krill, C. E. & Birringer, R. (1998). *Philos. Mag.* **77**, 621–640.
Langford, J. I. (1992). *Accuracy in Powder Diffraction II*. In *NIST Spec. Publ.* No. 846, edited by E. Prince & J. K. Stalick, pp. 110–126. Gaithersburg, MA: US Department of Commerce.
Langford, J. I. & Louër, D. (1982). *J. Appl. Cryst.* **15**, 20–26.
Langford, J. I., Louër, D. & Scardi, P. (2000). *J. Appl. Cryst.* **33**, 964–974.
Langford, J. I. & Wilson, A. J. C. (1978). *J. Appl. Cryst.* **11**, 102–113.
Leoni, M., Scardi, P. & Langford, J. I. (1998). *Powd. Diffr.* **13**, 210–215.
Louër, D., Auffrédic, J. P., Langford, J. I., Ciosmak, D. & Niepce, J. C. (1983). *J. Appl. Cryst.* **16**, 183–191.
Popa, N. C. (1998). *J. Appl. Cryst.* **31**, 176–180.
Scardi, P. & Leoni, M. (1999). *J. Appl. Cryst.* **32**, 671–682.
Scardi, P., Leoni, M. & Dong, Y. H. (2000). *Eur. Phys. J.* B**18**, 23–30.
Scardi, P., Leoni, M. & Dong, Y. H. (2001a). *Mater. Sci. Forum.* In the press.
Scardi, P., Leoni, M. & Dong, Y. H. (2001b). *CPD Newslett.* **24**, 23–24.
Scardi, P., Leoni, M. & Dong, Y. H. (2001c). In preparation.
Scherrer (1918). *Nachr. Ges. Wiss. Göttingen*, 26 September, pp. 98–100.
Snyder, R. L., Fiala, J. & Bunge, H. J. (1999). Editors. *Defect and Microstructure Analysis by Diffraction*. Oxford University Press.
Stokes, A. R. & Wilson, A. J. C. (1942). *Proc. Cambridge Philos. Soc.* **38**, 313–322.
Stokes, A. R. & Wilson, A. J. C. (1944). *Proc. Cambridge Philos. Soc.* **40**, 197–198.
Toraya, H. (1989). *Powd. Diffr.* **4**(3), 130–136.
Vargas, R., Louër, D. & Langford, J. I. (1983). *J. Appl. Cryst.* **16**, 512–518.
Warren, B. E. (1969). *X-ray Diffraction.* Reading, MA: Addison-Wesley.
Wilson, A. J. C. (1962). *X-ray Optics*, 2nd ed. London: Methuen.
Young, R. A. (1993). Editor. *The Rietveld Method.* Oxford University Press.